Tikrit Journal of Eng. Sciences/Vol.17/No.2/June 2010, (58-77)

# *Analytical Study Of Reinforced Concrete Continuous Deep Beams*

**Hosam A. Dahaam,** **Omer F. Ibraheem**
**Assistant Lecturer** **Assistant Lecturer**
**Civil Engineering Department, University of Tikrit**

**Abstract**

Nonlinear finite element analyses is carried out using the ANSYS11 program to predict the ultimate load for two different types of reinforced concrete continuous two-span deep beams. Results of comparing analytical with experimental data demonstrates the accuracy of the program. The effects of longitudinal reinforcement and web openings are studied and showed that the longitudinal reinforcement at top and middle region has little effect on the ultimate load, and the effect of web opening location has great effect on the ultimate load especially when the load path passes through the openings centerline. Web opening location also has great effect on values and distribution of shear and normal stresses especially at opening region.

**Key words: Deep Beam, Finite Element, Reinforced Concrete, Web opening**

## دراسة تحليلية للعتبات العميقة المستمرة

**الخلاصة**

تم إجراء التحليل بالعناصر المحددة باستخدام برنامج ANSYS11 لتتبع قيمة الحمل الأقصى لنوعين مختلفين من العتبات العميقة والمستمرة على فضائين. بينت نتائج المقارنة الدقيقة بين البيانات التحليلية النظرية والبيانات العملية دقة البرنامج. تمّ دراسة تأثير التسليح الطولي وفتحات الوترة وقد أظهرت الدراسة بأن التسليح الطولي في أعلى العتبة وفي وسطها له تأثير محدود على قيمة الحمل الأقصى وتأثير موقع فتحات الوترة له تأثير كبير جدا على الحمل الأقصى خصوصا عند مرور مسار الحمل خلال مركز ثقل الفتحة. بينت النتائج أيضا ان لموقع الفتحة تأثيرا كبيرا على قيم وتوزيع الاجهادات العمودية واجهادات القص خاصة عند منطقة وجود الفتحة.

**الكلمات الدالة: عتبة عميقة، عناصر محددة، خرسانة مسلحة، فتحة الوترة**

**Notation**

[*B*] Strain displacement matrix.
*{d}* Nodal displacement vector.
$\{d^*\}_e$ Column vector of virtual nodal displacements.
$\{d\}_e$ Column vector of nodal displacements
[*D*] Constitutive law matrix.
*{f}* Nodal force vector.
$K_e$ Element stiffness matrix.
[*L*] Differential operator matrix.
[N] Shape function matrix.
$\{U\}_e$ Displacement vector at any point within the element.
*u, v, w* The displacement components

***Greek letters***

$\{\sigma\}_e$ Axial stress vector.
$\{\varepsilon\}$ Nodal strain vector.
$\{\varepsilon\}_e$ Column vector of nodal strains

**Introduction**

A deep beam is a beam in which significant amount of load is carried to

Tikrit Journal of Eng. Sciences/Vol.17/No.2/June 2010, (58-77)

the supports by a compression thrust joining the load and the reaction. This occurs if a concentrated load acts closer than about (2d) to the support, or for uniformly loaded beams with a span-to-depth ratio ($l_n$/d) less than about 4 to 5[1].

Most typically deep beams occurs as transfer girders which may be single span or continuous. A transfer girder supports the load from one or more columns, transferring it laterally to other columns. Deep beams action also occurs in some walls and in pile caps.

**Behavior of Deep Beams**

Elastic analyses of deep beams in the uncracked state are only meaningful prior to cracking. In deep beams, cracking will occur at one-third to one-half of the ultimate load. After cracks is developed, a major redistribution of stresses is necessary since there can be no tension across the cracks. The results of elastic analysis are of interest primarily because they show the distribution of stresses which cause cracking and hence give guidance as to the direction of cracking and the follow of forces after cracking. In Figure (1), the dashed lines are compressive stress trajectories parallel to the directions of the principal compressive stresses, and the solid lines are tensile stress trajectories parallel to the principal tensile stresses. Cracks would be expected to occur perpendicular to the solid lines[2].

Stresses in deep beams before cracking can be studied using the methods of two-dimensional elasticity or the finite element method. Such studies show that the plane section before bending do not necessarily remain plane after bending. Significant warping of cross-section occurs because of high shear stresses. The resulting strain distribution is no longer considered as linear and shear deformations that are neglected in normal beams become significant. Hence, flexural stresses are not linearly distributed even in the elastic stage and the usual methods for calculating section properties and stressed can not be applied.

**Strut-and-Tie Action**

Large portion of compressive force is directly transferred to supports by the strut-and-tie action. Strut-and-tie action is a system of forces in equilibrium with a given set of loads. It consists of concrete compressive struts, reinforcing bars as tension ties, and joints or nodal zones[1].

The available strength from strut-and-tie action is largely dependent on whether the resulting diagonal compression stress can be accommodated. Deep or short beams develop inclined cracks, which is able to carry additional load by compressive strut. Significant part of the load is transferred directly from the point of applied load to the support by this diagonal compressive strut. The horizontal compression in concrete and the tension in the main reinforcement have to equilibrate the load. The geometry of this mechanism, which contributes shear strength, is clearly depending on placement of the loads and reactions. Strut-and-tie will be formed after diagonal cracking appears, even though diagonal tension failure mode occurs in the slender beams. Deep beams carry more loads after diagonal cracking due to the behavior of strut-and-tie. Figure (2) shows a strut-and-tie model for a two-span continuous deep beam. At the interior support, two struts carry the load. The upper truss shown in Figure (2a) utilizes the bottom reinforcement, and the lower truss shown in Figure (2b) uses the bottom reinforcement, while

Tikrit Journal of Eng. Sciences/Vol.17/No.2/June 2010, (58-77)

Figure (2c) shows the complete plastic truss[1].

**Relative Previous Studies**

Rogowsky, et al.[3] tested seven simply supported and seventeen two span deep beams under concentrated loads. The tested specimens are divided into three series of similar a/d ratio (shear span/depth of beam). Typical series consisted of seven beams having different reinforcement patterns. They concluded that the behavior ranged from brittle for beams without vertical web reinforcement to ductile for beams with large amount of vertical web reinforcement. The horizontal web reinforcement has no effect on the ultimate capacity.

Tan et al. [4] undertook a study on the shear strength of nineteen deep beams with concrete compressive strengths from 41 to 59 MPa. Test results indicated that the shear span to depth ratio has a significant effect on the ultimate strength. In comparing test results with predictions based on the ACI 318-89 Building Code showed that the code equations can be used for designing deep beams with concrete compressive strength in the range mentioned earlier, but the equations can be very conservative at low a/d ratios.

Shah and Mishra[5] reported results of tests on twelve simply supported deep beams under single point loading with steel fibers of 0.45 mm diameter. The ratio of steel fibers is 1.0% by volume from the concrete mix. It is concluded that the inclusion of steel fibers in the concrete deep beam resulted in reduced crack width and deflection at all stages of loading through to failure. Fiber reinforcement can increase the stiffness of concrete, also increasing the ductility

Mansur and lee[6] developed an ultimate strength model for reinforced concrete beams that contain large opening and subjected to a point load. The model predicted that the ultimate strength of a beam decreases with an increase in opening size and also with increasing moment to shear ratio at the center of opening. The strength decreases at the opening eccentricity below the beam axis increase.

Haque, Rasheeduzzafar, and Al-Tayyib[7] tested twelve deep beams using photo elastic technique to establish the effects on the nature and magnitude of stress distribution of the beam dimensional parameters L/d ratio, presence of openings, and the position of the opening. It is concluded that, in deep beams with web openings, the pattern of stress flow is different from solid web beams only locally around openings. The effect of web openings in terms of increasing the critical flexural tensions was found to be significant only in shallower beams and become negligible for deeper beams. Regions of high critical diagonal tensions appear above and around the corners of the openings. Openings should be located away from the loaded quadrants of high shear zone to obtain higher beam strength.

Khalf[8] presented a non-linear analysis of reinforced concrete deep beams under monotonically increasing load using the finite element technique. Concrete is represented by eight-node plane stress isoparametric elements for the two-dimensional finite element analysis and by twenty-node brick element for the three-dimensional finite element analysis. Bar elements are used to represent the reinforcement in two-dimensional analysis, and membrane elements are used to model the reinforcement in the three-dimensional analysis.

Samir and Chris[9] describes a series of nonlinear finite element analyses carried out using the commercial package, DIANA7 to predict the

ultimate load and mode of failure for three different types of reinforced concrete continuous two-span deep beams. Only one parameter, the shear retention factor, was varied during the analysis. They concluded that the finite element method is capable of modeling the behavior of the reinforced concrete deep beams, and the predictions of the ultimate load are within an accuracy region of 5%.

**Finite Element Generation**

The ultimate purpose of a finite element analysis is to recreate mathematically the behavior of an actual engineering system. In other words, the analysis must use an accurate mathematical model of the physical prototype. In the broadest sense, this model comprises all the nodes, elements, material properties, real constants, boundary conditions, and other features that are used to represent the physical system.

In ANSYS11 terminology, the term model generation usually takes on the narrower meaning of generating the nodes and elements that represent the spatial volume and connectivity of the actual system. Thus, model generation in this discussion will mean the process of defining the geometric configuration of the model's nodes and elements[10].

**Basic Finite Element Relationships**

The basic steps are the derivation of the element stiffness matrix, which relate the nodal displacement vector, *{d}*, to the nodal force vector,*{f}*.

Considering a body subjected to a set of external forces, the displacement vector at any point within the element $\{U\}_e$ is given by:

$$\{U\}_e = [N].\{d\}_e \quad \text{.....(1)}$$

where, [N] is the matrix of shape functions, $\{d\}_e$ the column vector of nodal displacements. The strain at any point can be determined by differentiating Eq. (1):

$$\{\varepsilon\}_e = [L].\{U\}_e \quad \text{.....(2)}$$

where, [L] is the matrix of differential operator. In expanded form, the strain vector can be expressed as:

$$\{\varepsilon\} = \begin{Bmatrix} \varepsilon_x \\ \varepsilon_y \\ \varepsilon_z \\ \gamma_{xy} \\ \gamma_{yz} \\ \gamma_{zx} \end{Bmatrix} = \begin{Bmatrix} \dfrac{\partial u}{\partial x} \\ \dfrac{\partial v}{\partial y} \\ \dfrac{\partial w}{\partial z} \\ \dfrac{\partial u}{\partial y} + \dfrac{\partial v}{\partial x} \\ \dfrac{\partial v}{\partial z} + \dfrac{\partial w}{\partial y} \\ \dfrac{\partial w}{\partial x} + \dfrac{\partial u}{\partial z} \end{Bmatrix} \quad \text{.....(3)}$$

Substituting Eq (1) into Eq.(2) gives:

$$\{\varepsilon\}_e = [B].\{d\}_e \quad \text{.....(4)}$$

Where: [B] is strain-nodal displacement matrix given by:

$$[B] = [L].[N] \quad \text{.....(5)}$$

The stress vector can be determined using the appropriate stress-strain relationship as:

$$\{\sigma\}_e = [D].\{\varepsilon\}_e \quad \text{.....(6)}$$

where, [D] is the constitutive matrix and $\{\sigma\}_e$ is:

$$\{\sigma\}_e = \begin{bmatrix} \sigma_x & \sigma_y & \sigma_z & \tau_{xy} & \tau_{yz} & \tau_{zx} \end{bmatrix}^T \quad \text{.....(7)}$$

From Eqs. (4 & 5), the stress-nodal displacement relationship can be expressed as:

$$\{\sigma\}_e = [D].[B].\{d\}_e \quad \ldots\ldots\ldots\ldots\ldots\ldots(8)$$

To write the force- displacement relationship, the principal of virtual displacements is used. If any arbitrary virtual nodal displacement, $\{d^*\}_e$, is imposed, the external work, $W_{ext.}$, will be equal to the internal work $W_{int.}$:

$$W_{ext.} = W_{int} \quad \ldots\ldots\ldots\ldots\ldots\ldots(9)$$

In which:

$$W_{ext.} = \{d^*\}_e^T.\{f\}_e \quad \ldots\ldots\ldots\ldots\ldots\ldots(10)$$

And

$$W_{int.} = \int_v \{d^*\}_e^T.\{\sigma\}_e.dv \quad \ldots\ldots\ldots\ldots\ldots(11)$$

Where, $\{f\}_e$ is the nodal force vector.
Substituting Eq.(4) into Eq.(11), gives:

$$W_{int} = \{d^*\}_e^T.\int_v [B]^T.\{\sigma\}_e.dv \quad \ldots\ldots\ldots\ldots(12)$$

From Eqs. (8 & 12),

$$W_{int} = \{d^*\}_e^T.\int_v [B]^T.[D].[B].dv.\{d\}_e \quad \ldots(13)$$

and Eq. (9) can be written as :

$$\{d^*\}_e^T.\{f\}_e = \{d^*\}_e^T.\int_v [B]^T.[D].[B].dv.\{d\}_e \quad \ldots 14)$$

or

$$\{f\}_e = \int_v [B]^T.[D].[B].dv.\{d\}_e \quad \ldots\ldots\ldots(15)$$

letting:

$$[K]_e = \int_v [B]^T.[D].[B].dv \quad \ldots\ldots\ldots\ldots\ldots(16)$$

Then

$$\{f\}_e = [K]_e.\{d\}_e \quad \ldots\ldots\ldots\ldots\ldots\ldots(17)$$

where, $[K]_e$ is the element stiffness matrix.
Thus, the overall stiffness matrix can be obtained by:

$$[K] = \sum_n \int_v [B]^T.[D].[B].dv \quad \ldots\ldots\ldots\ldots(18)$$

Ttotal external force vector $\{f\}$ is then:

$$\{f\} = [K].\{d\} \quad \ldots\ldots\ldots\ldots\ldots\ldots\ldots(19)$$

where, $\{d\}$ is the unknown nodal point displacements vector[11].

**Solid 65 Element Description**

In ANSYS11 program, SOLID65 (or 3-D reinforced concrete solid) is used for the 3-D modelling of solids with or without reinforcing bars (rebar). The solid is capable of cracking in tension and crushing in compression. In concrete applications, for example, the capability of the solid element may be used to model the concrete, while the rebar capability is available for modeling reinforcement behaviour. The element is defined by eight nodes having three degrees of freedom at each node: translations of the nodes in x, y, and z-directions. Up to three different rebar specifications may be defined.

The most important aspect of this element is the treatment of nonlinear material properties. The concrete is capable of cracking (in three orthogonal directions), crushing, plastic deformation, and creep. This 8-node brick element is used, in this study to simulate the behaviour of concrete layer. The element is defined by eight nodes and by the isotropic material properties. The geometry, node locations, and the coordinate system for this element are shown in Figure (3)[10].

For this element, the displacement field is represented by:

$$u(r,s,t) = \sum_{i=1}^{8} N_i(r,s,t).u_1 \quad \ldots\ldots\ldots\ldots(20)$$

$$v(r,s,t) = \sum_{i=1}^{8} N_i(r,s,t).v_1 \quad \ldots\ldots\ldots\ldots(21)$$

$$w(r,s,t)=\sum_{i=1}^{8} N_i(r,s,t).w_1 \ldots\ldots\ldots..(22)$$

Where: $u_i$, $v_i$ and $w_i$ are the displacement components of node i, and Ni (r,s,t) is the shape function at node i,

$$N_i(r,s,t)=\frac{1}{8}(1+r.r1).(1+s.s1).(1+t.t1)$$
$$.(r.r1+s.s1+t.t1-2) \ldots\ldots\ldots\ldots\ldots...(23)$$

Where: $r_i = \pm 1$, $s_i = \pm 1$, $t_i = \pm 1$

**LINK 8 Element Description**

LINK8 is a spar (or truss) element which may be used in ANSYS11 program in a variety of engineering applications. This element can be used to model trusses, sagging cables, links, springs, etc. The 3-D spar element is a uniaxial tension-compression element with three degrees of freedom at each node: translations of the nodes in x, y, and z-directions. As in a pin-jointed structure, no bending of the element is considered. Plasticity, creep, swelling, stress stiffening, and large deflection capabilities are included. This element is used to simulate the behaviour of reinforcement bars and thus it is capable of transmitting axial forces only. The geometry, node locations, and the coordinate system for this element are shown in Figure (4)[10].

Also, Solid65 element can be used to analyze problems with reinforced bars. Up to three rebar specifications may be defined. The rebars are capable of plastic deformation and creep. The rebar orientation is defined by two angels measured with respect to the element's coordinate system (see Fig. 3)

**Experimental Verification**

To ascertain the validity of th proposed element, two continuous dee beams are analyzed. These beams are tested by others and sufficient experimental data is available for their proper modeling by the finite element method.



**The Finite Element Program Used:**

The finite element package ANSYS11 program has been applied to estimate the ultimate load and the mode of failure for a reinforced concrete two span continuous deep beams under consideration.

**Experimental Beams**

Samir and Chris[9] tested a series of continuous two span deep beams. Here two types of beams will be analyze. The two were identical in geometry and longitudinal reinforcement, and had a thickness of 90 mm and dimensions as shown in Figure (5). The differences between the two beams were in the vertical reinforcement patterns and the concrete properties. Beam S1 has no vertical stirrups while the second beam S2 has 8 mm diameter stirrups at 130 mm spacing.

Table (1) gives the material properties used in the analysis of the two beams.

**Results and Discussion**

Results of the analysis are shown in Figs. (7 & 8). Figure (7) shows the load mid-span deflection curve of beam S1 while Figure (8) illustrates the load mid-span deflection of beam S2. As can be seen from Figure (7), a reasonable agreement between the computed and experimental values is obtained. The ultimate load is accurately predicted but the finite element response is a little stiffer. The results in Figure (8) for beam S2 shows good agreement between the computed and experimental values.

***Effect of Longitudinal Reinforcement***

Longitudinal reinforcement used by Samir and Chris[9] is studied here. The longitudinal reinforcement areas at bottom, middle, and top are changed to investigate its effect on beam capacity.

Figure (9 & 10) show the effect of bottom longitudinal reinforcement on deep beam nonlinear response. The beam behaves more ductile at low percentage of steel reinforcement especially for beams without stirrups, and an increase in load capacity of 16 % due to increasing in steel area of 90 %, while an increase in load capacity of 30% for beam with vertical reinforcement is noticed.

Middle reinforcement has low effect on the load capacity of deep beam. Figures (11&12) show that an increase in steel area of 85 % causes increasing in ultimate load of 15 % for beam with vertical stirrups.

Top reinforcement also has very small effect on the ultimate load of continuous deep beam as shown in Figures(13 & 14). An increase in reinforcing area of 85 % causes load capacity increase of 9 %.

### *Effect of Web Openings*

Web opening effects also studied here for beams S1 and S2 under the effect of various opening layout shown in Figure (6). The openings decreases the ultimate strength of deep beams since the openings decreases the concrete strength by decreasing the concrete section. However, it is found that the position of the opening has wide effect on the ultimate load capacity. When the load path do not pass through the centre of the opening as in layout No.1 (Figure 6), a reduction in ultimate capacity is very small especially for deep beam with stirrups, as shown in Figs. (15 & 16). But, when the load path for the exterior supports passes through the centre of the opening as in layout No.2, 3, and 4, a reduction in the ultimate capacity is obvious when the openings is at top, middle, and bottom reinforcement regions as shown in Figs. (17 to 22). High reduction in ultimate load capacity of about 40% compared with solid beam is observed when the load path from interior support passes through the centre of the opening –layout No.5- for beam without stirrups while a reduction of 25% for beam with vertical stirrups as shown in Figs. (23 & 24). This behavior is due to the strut-and-tie action of the beam. Figures (25 & 26) also show the effect of four openings on the continuous beam –layout No.6.

### *Stresses in Concrete*

Normal and shear stresses at the opening sections are calculated throughout the beam depth and at stages just before and after concrete cracking for opening patterns no.2, 3, 4 and 5 only.

Normal stress for opening layout No.2, has nearly same behavior for solid and opened case, Figs. (27 & 28). For other opening layout, there are a great effect for opening. Stresses values at opening edges are increased especially for layout No.4 opening near exterior reaction-except that for opening layout No.2 (See Figs. 29 - 34). A great difference in stress distribution between solid and opened beams can be noted at cracking stage (Figs. 35 - 42).

Shear stresses for solid beams differs in behavior from that with opening except for opening pattern No.2. before crack only. Values of shear stress is increased at opening edges and layout No.4 have the greatest value ( Figs.43-58). Generally, stirrups reinforcement increases shear and normal stress capacity in concrete especially after cracking.

## Conclusions and Recommendations

**1.**The finite element method which is represented by the ANSYS11 program is capable of modeling the behavior of the reinforced concrete continuous deep beams.

**2.**The program yields good results as demonstrated by the analysis of two beams. Longitudinal reinforcement at top and middle regions has very little effect on the behavior of continuous deep beams, while the bottom reinforcement has an effective effect on the beam.

**3.**Web opening location has great effect on the ultimate capacity of continuous deep beam especially when the load path passes through the centre of the opening.

**4.**An increase in stresses values at opening edges can be noted clearly, and opening layout also has great effect on values and distribution of that stresses.

Further studies is needed to verify the behavior of continuous deep beams under different loading conditions, also the effect of dynamic loading and the effect of web opening shape have to studied.

**References**

**1.** James G. MacGregor "Reinforced Concrete Mechanics and Design" Prentice Hall International Series, 3rd Edition, 1998.

**2.** David M. Rogowsky and James G. Mac Gregor, "Design of Deep Reinforced Concrete Continuous Beams", Concrete International Design and Construction, Vol.8, No. 8, Aug. 1986, P.P. 49-58.

3. Rogowsky, D.M., Mac Gregor, J.G., and Ong, S.Y.,"Test of Reinforced Concrete Deep Beams", ACI Journal, Vol. 83, No. 4, July-Aug. 1986, P.P. 614-623.

**4.** Tan, k.H., Kong F.K., Teng S. and Guan L., "High Strength Concrete Deep Beams With Effective Span and Shear Span Variations", ACI Journal, Proceedings Vol. 92 No. 4, July-Aug. 1995, P.P. 395-465.

**5.** Shah, R.H., and Mishra, S. V., "crack and Deformation Characteristic of SFRC Deep Beams", IE Journal, Vol. 85, May 2004, P.P. 44-48.

**6.** Mansur, M.A. and Lee, S.C., " Collapse Loads of Reinforced Concrete Beams With LargeOpenings", ASCE Journal of Structural Engineering, Vol. 110, No. 11, Nov. 1984, P.P. 2603-2618.

**7.** Haque, M., Rasheeduzzafar, and Al-Tayyib, A. H. J., " Stress Distribution in Deep Beams With Web openings", ASCE Journal of Structural Engineering, Vol. 112, No. 5, May 1986, P.P. 1147-1165.

**8.** Khalaf, I.M., "Non-Linear Finite element Analysis of Reinforced Concrete Deep Beams", M.Sc. thesis, University of Mosul, 1992.

**9.** Samir M. O. Dirar and Chris T. Morley, " Nonlinear Finite Element Analysis of Reinforced Concrete Deep Beams", International Conference on computational Plasticity, Barcelona 2005.

**10.**Saeed Moaveni "Finite Element Analysis Theory and Application With ANSYS", Prentice Hall International Series, 3rd Edition, 2008.

**11.**Kenneth H. Huebner, Donald L. Dewhirst, Douglas E. Smith and Ted G. Byrom "The Finite Element Method For Engineers", John Wiley & Sons, 2nd Edition, 2004.

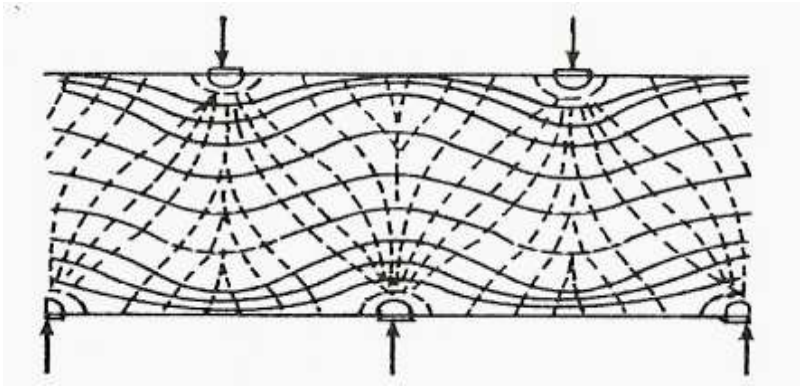

**Figure (1) Stress Trajectories of Multi-Span Deep Beam[1].**

(a)

(b)

(c)

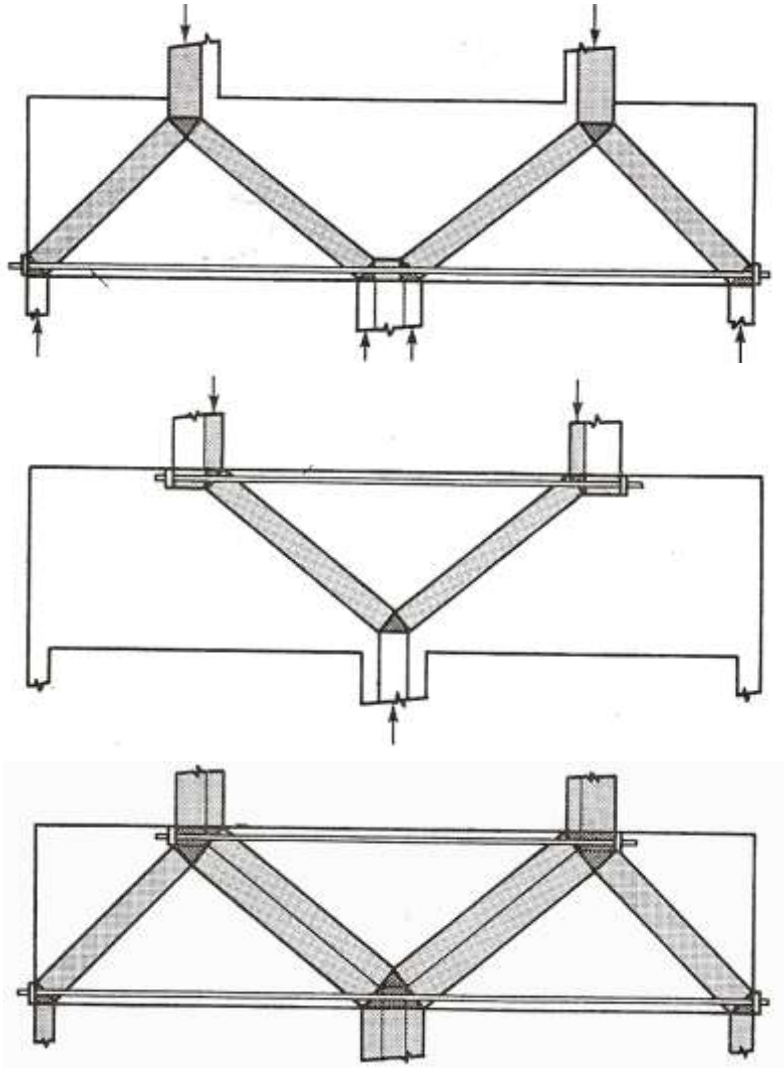

**Figure (2) Strut-and-Tie Model for a Two-Span Continuous Beam[1].**
**(a) Positive Moment Truss. (b) Negative Moment Truss. (c) Complete Plastic Truss.**

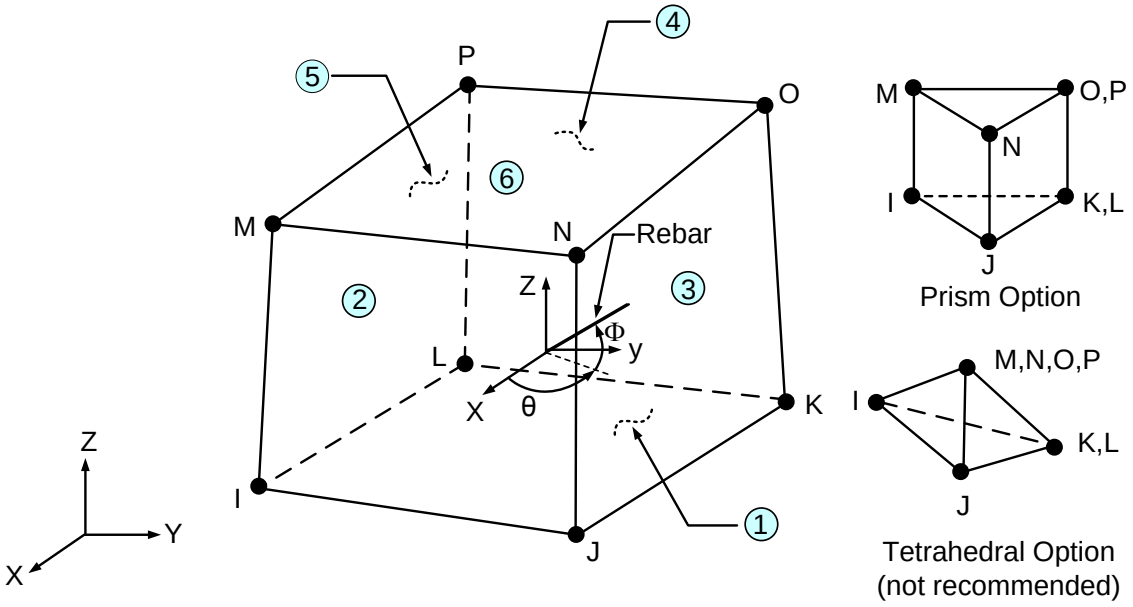


**Figure (3) SOLID65 Geometry[10].**

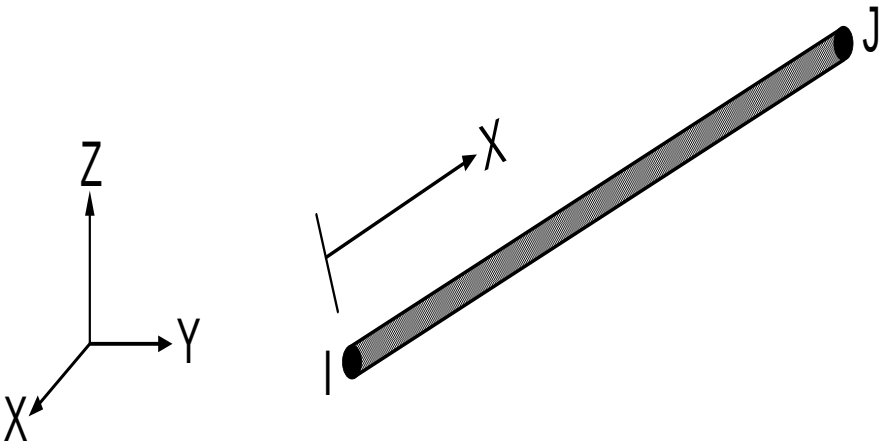


**Figure (4) LINK8 Geometry [10]**

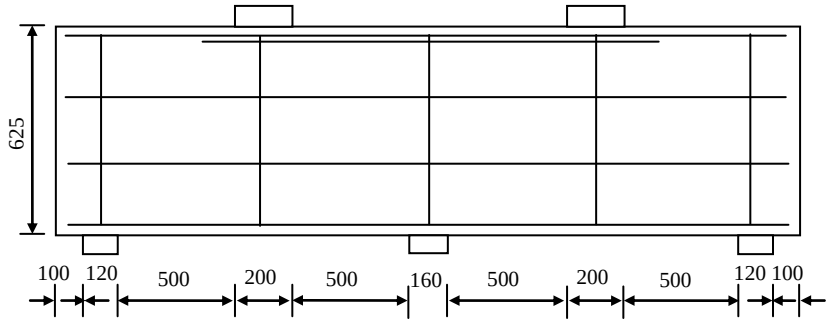


**All dimensions in (mm)**

**Figure (5) Samir and Chris Continuous Deep Beam Tested[9].**

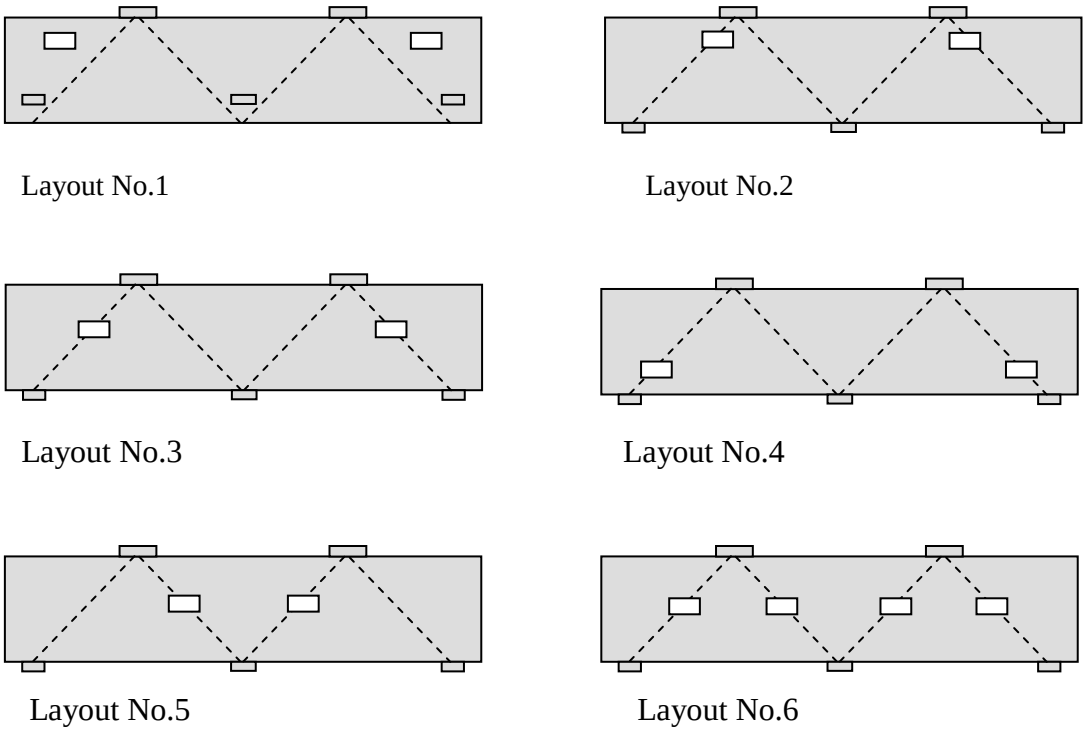


**Fig. (6) Beam Opening Layout.**

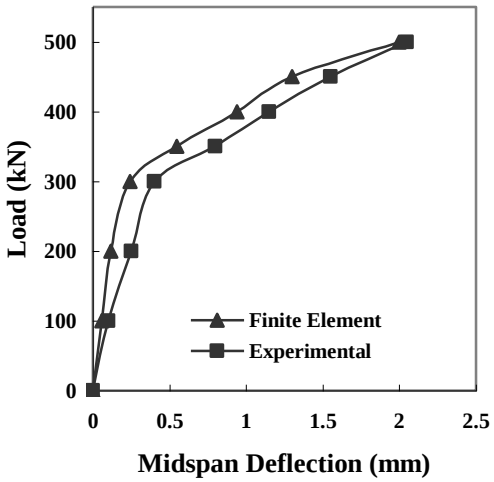


Fig. (7) Load Deflection Curves For Beam S1.

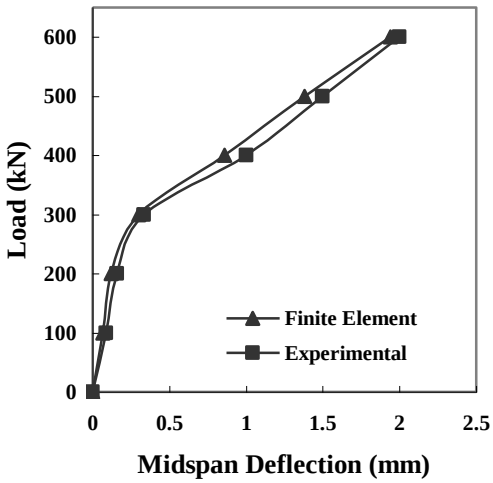


Fig. (8) Load Deflection Curves For Beam S2

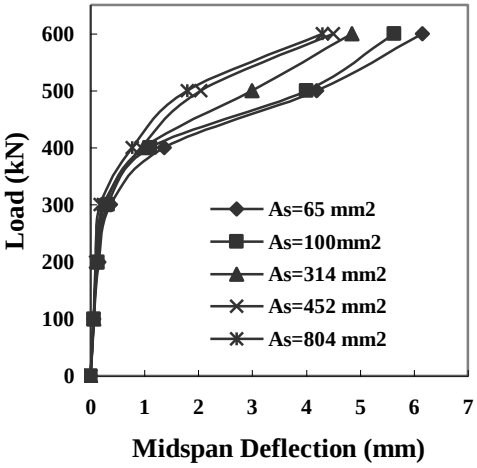


Fig. (9) Load Deflection Curves For Beam S1.

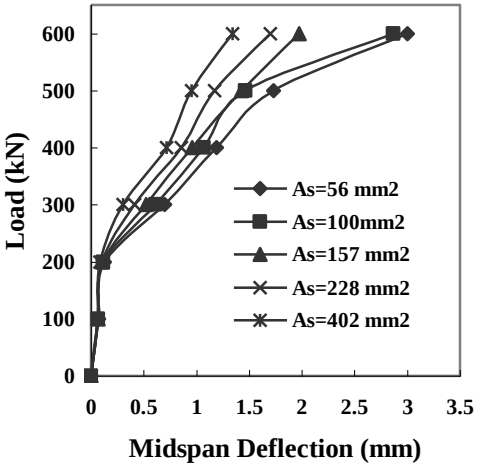


Fig. (10) Load Deflection Curves For Beam S2.

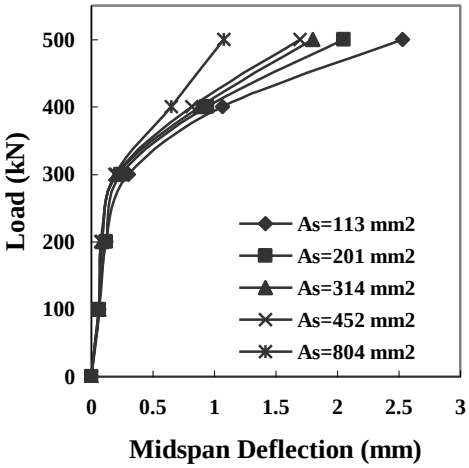


Fig. (11) Load Deflection Curves For Beam S1.

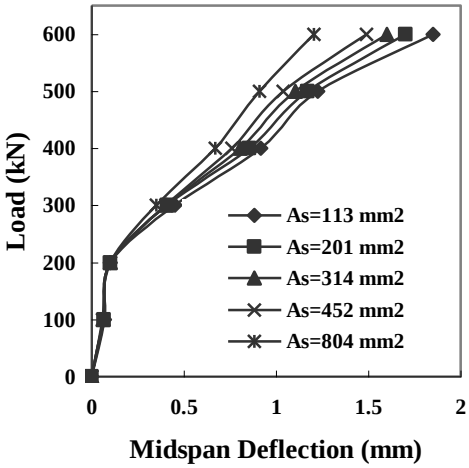


Fig. (12) Load Deflection Curves For Beam S2.

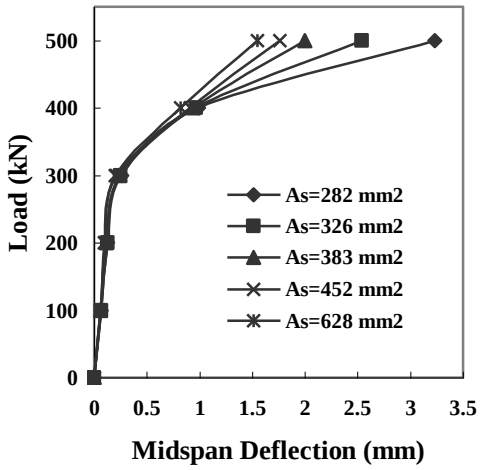


Fig. (13) Load Deflection Curves For Beam S1.

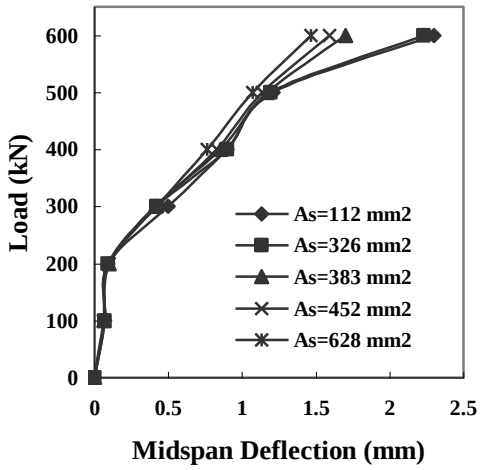


Fig. (14) Load Deflection Curves For Beam S2.

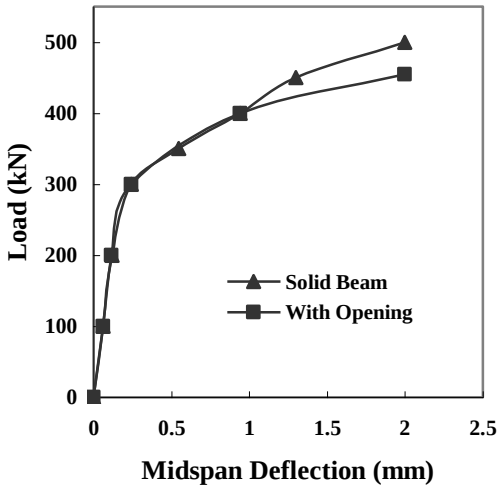


Fig. (15) Load Deflection Curves for Beam S1 and Opening Layout No.1

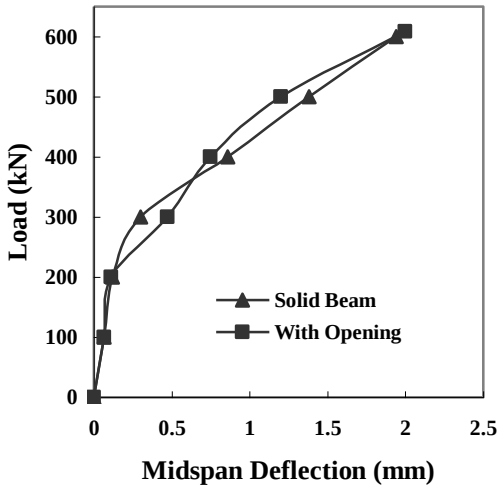


Fig. (16) Load Deflection Curves for Beam S2 and Opening Layout No.1

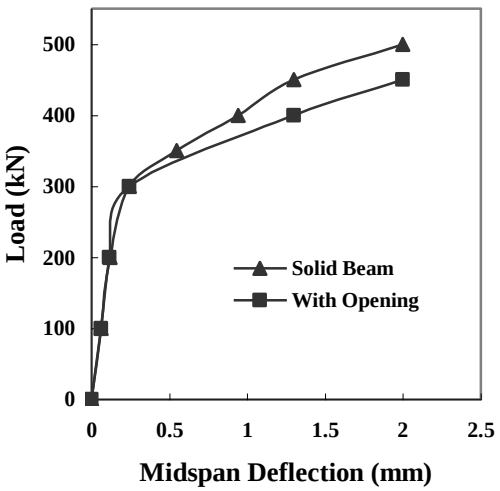


Fig. (17) Load Deflection Curves for Beam S1 and Opening Layout No.2

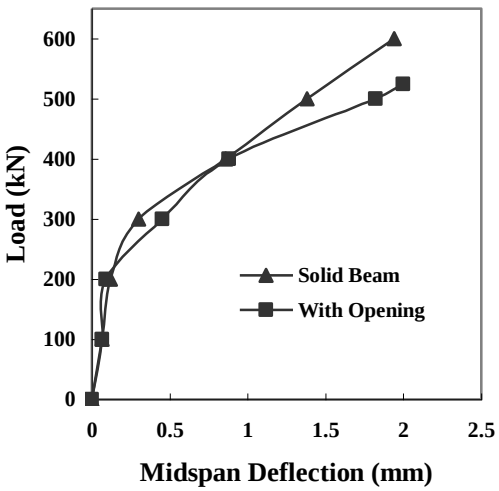


Fig. (18) Load Deflection Curves for Beam S2 and Opening Layout No.2

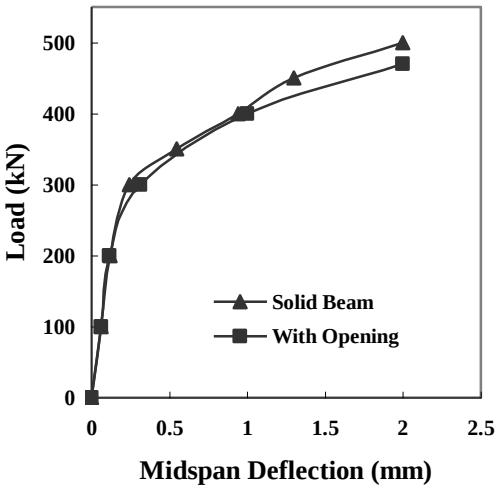


Fig. (19) Load Deflection Curves for Beam S1 and Opening Layout No.3

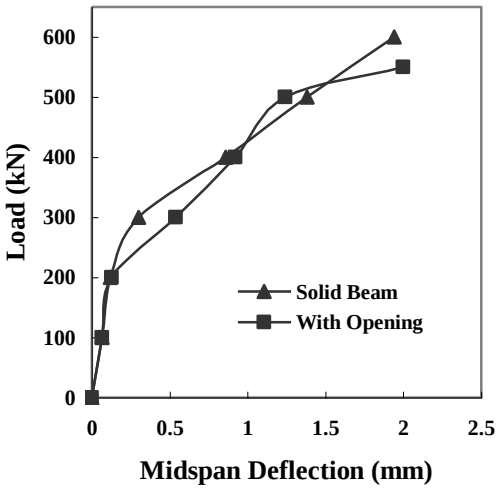


Fig. (20) Load Deflection Curves for Beam S2 and Opening Layout No.3

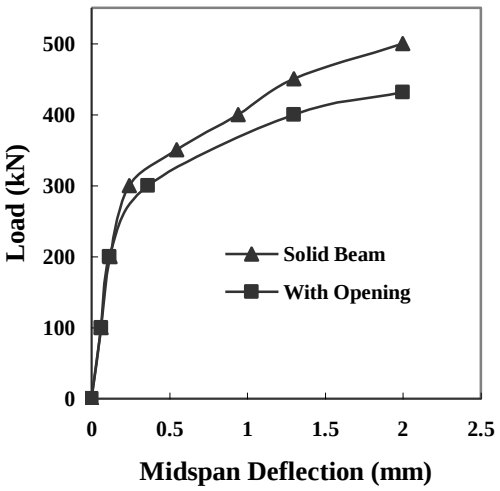


Fig. (21) Load Deflection Curves for Beam S1 and Opening Layout No.4

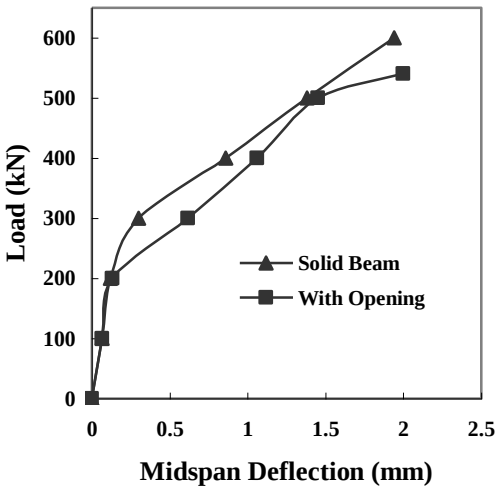


Fig. (22) Load Deflection Curves for Beam S2 and Opening Layout No.4

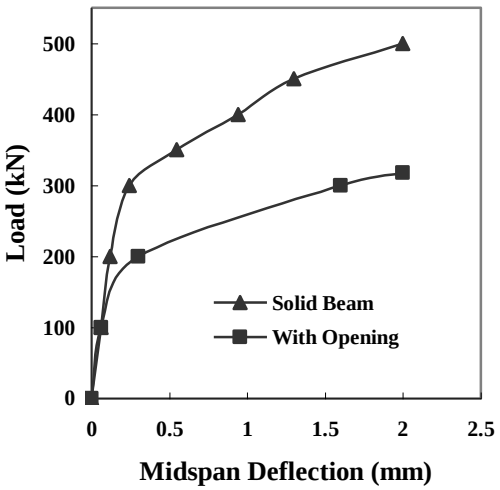


Fig. (23) Load Deflection Curves for Beam S1 and Opening Layout No.5

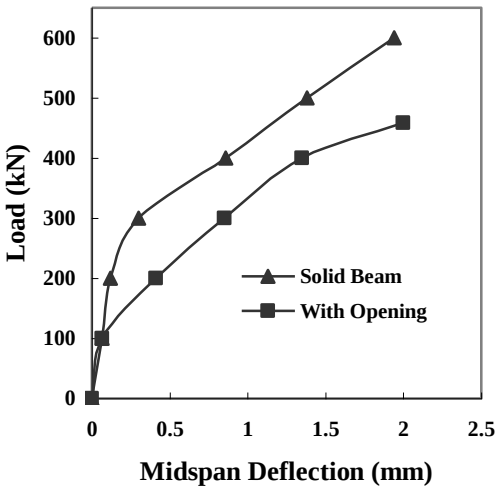


Fig. (24) Load Deflection Curves for Beam S2 and Opening Layout No.5

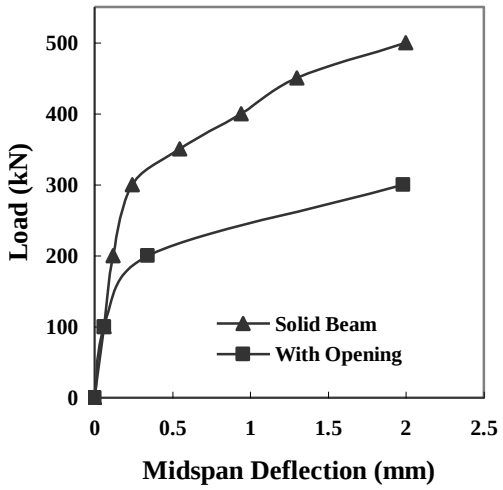


Fig. (25) Load Deflection Curves for Beam S1 and Opening Layout No.6

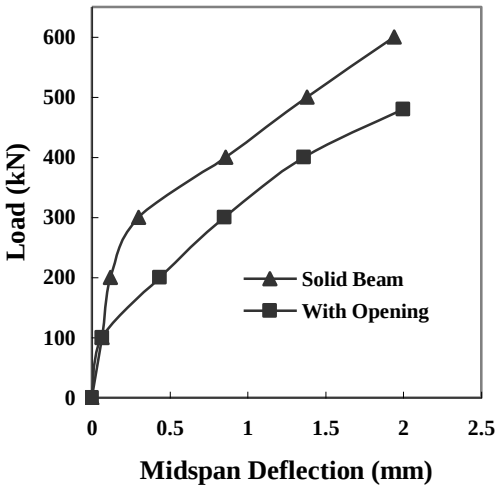


Fig. (26) Load Deflection Curves for Beam S2 and Opening Layout No.6

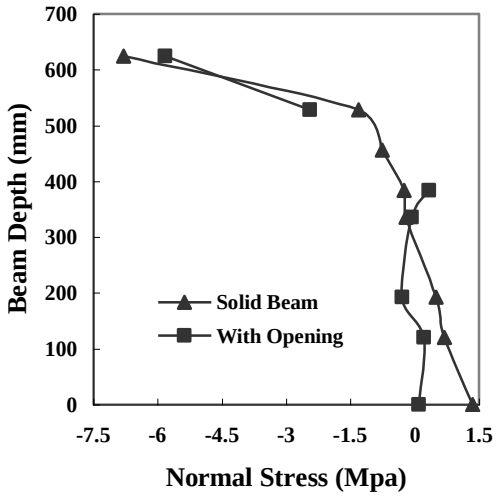


Fig. (27) Normal Stress for Beam S1 at Opening Layout No.2

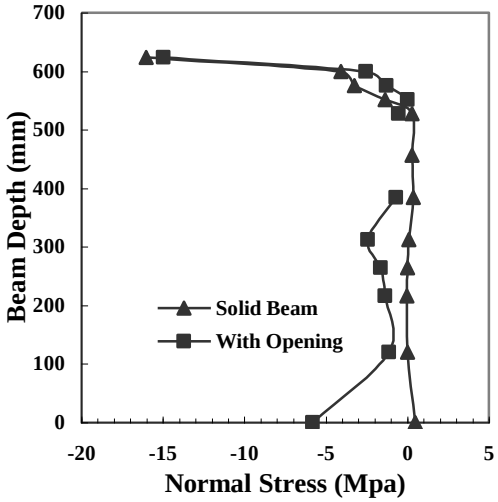


Fig. (28) Normal Stress for Beam S2 at Opening Layout No.2

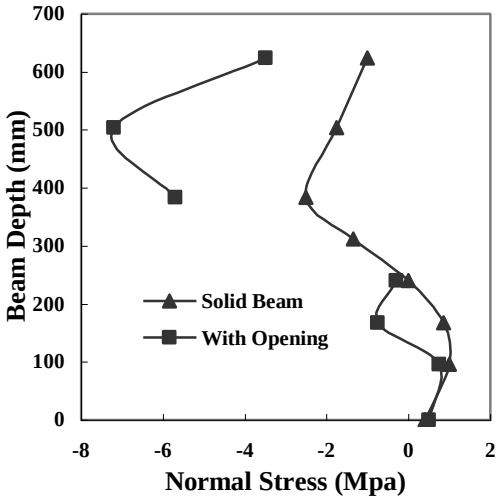


Fig. (29) Normal Stress for Beam S1 at Opening Layout No.3

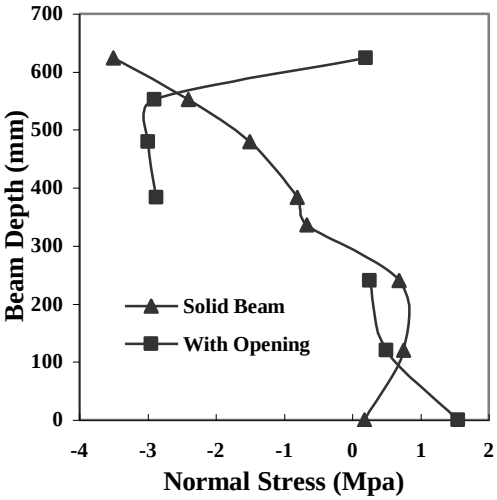


Fig. (30) Normal Stress for Beam S2 at Opening Layout No.3

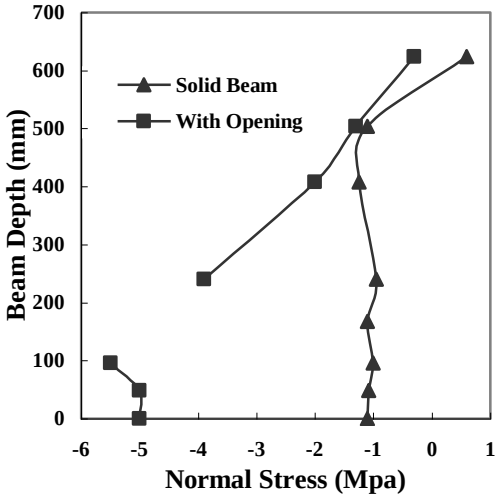


Fig. (31) Normal Stress for Beam S1 at Opening Layout No.4

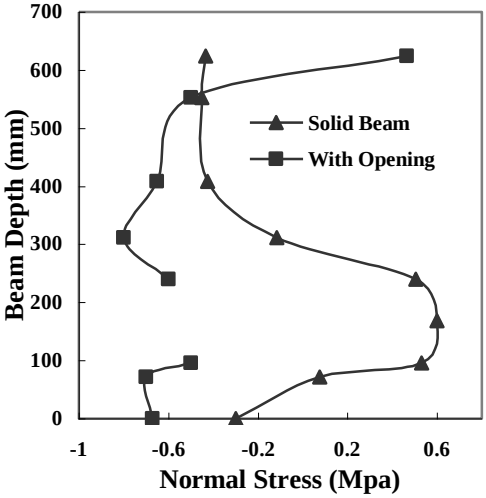


Fig. (32) Normal Stress for Beam S2 at Opening Layout No.4

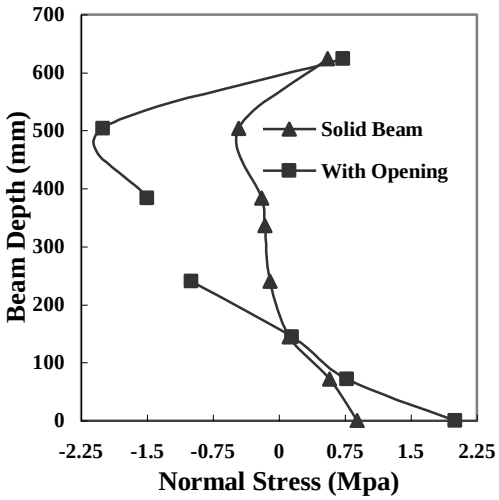


Fig. (33) Normal Stress for Beam S1 at Opening Layout No.5

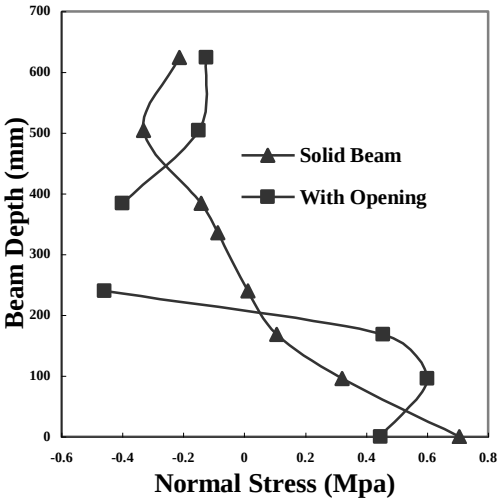


Fig. (34) Normal Stress for Beam S2 at Opening Layout No.5

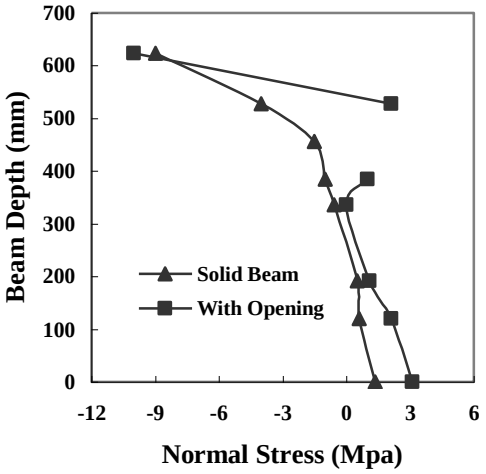


Fig. (35) Normal Stress for Beam S1 at Opening Layout No.2 After Crack

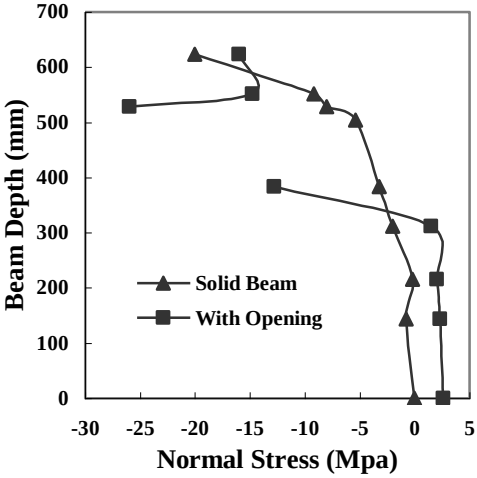


Fig. (36) Normal Stress for Beam S2 at Opening Layout No.2 After Crack

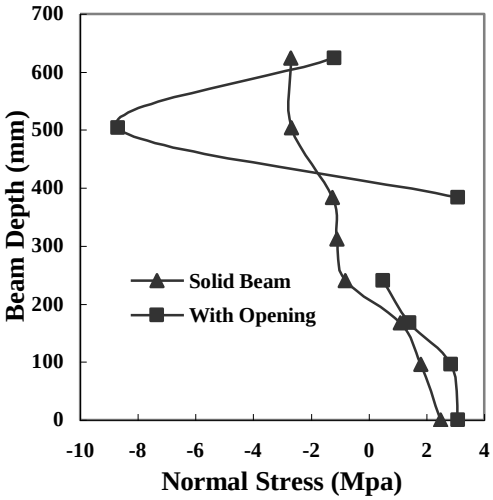


Fig. (37) Normal Stress for Beam S1 at Opening Layout No.3 Afters Crack

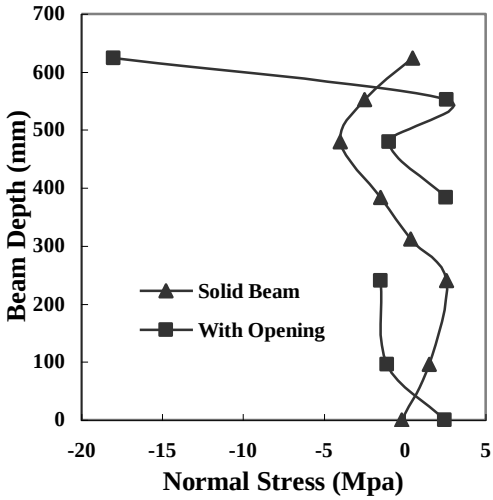


Fig. (38) Normal Stress for Beam S2 at Opening Layout No.3 After Crack

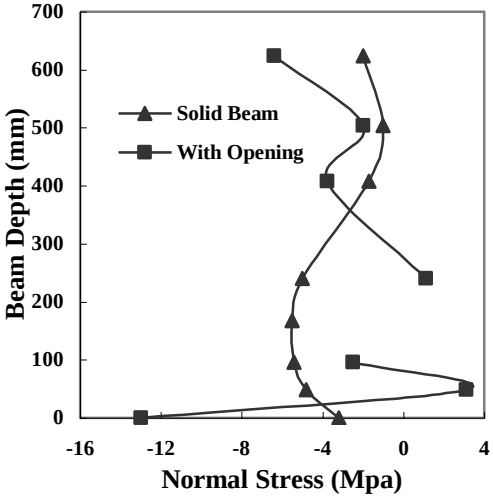


Fig. (39) Normal Stress for Beam S1 at Opening Layout No.4 After Crack

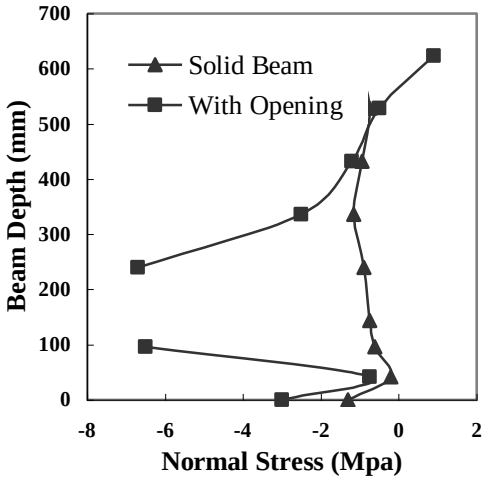


Fig. (40) Normal Stress for Beam S2 at Opening Layout No.4 After Crack

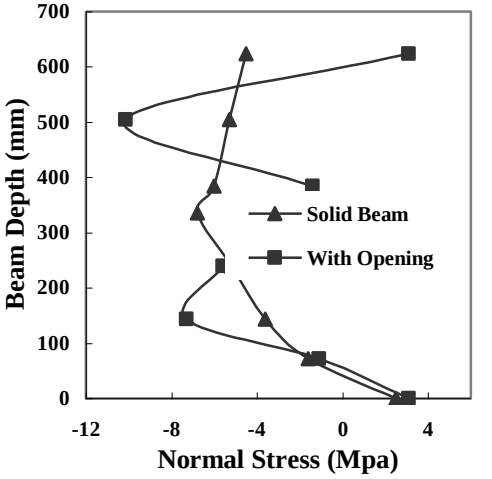


Fig. (41) Normal Stress for Beam S1 at Opening Layout No.5 After Crack

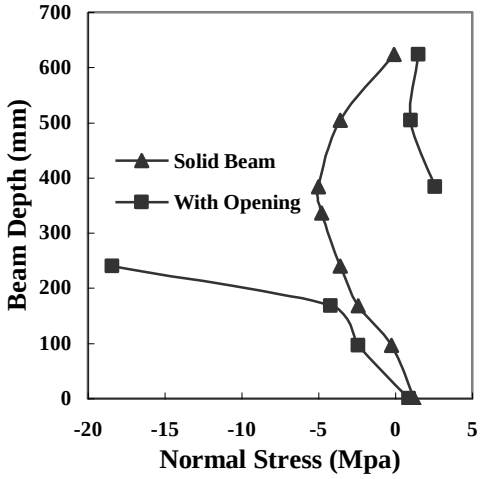


Fig. (42) Normal Stress for Beam S2 at Opening Layout No.5 After Crack

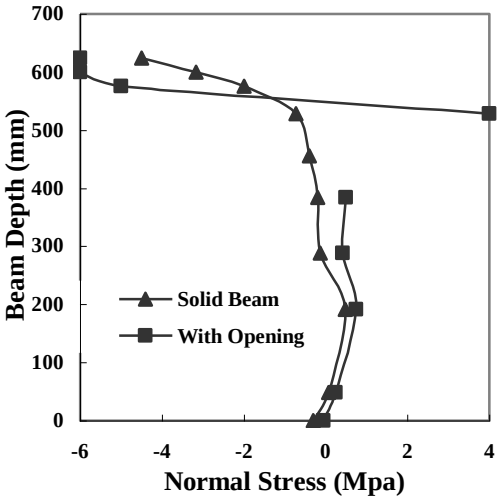


Fig. (43) Shear Stress for Beam S1 at Opening Layout No.2

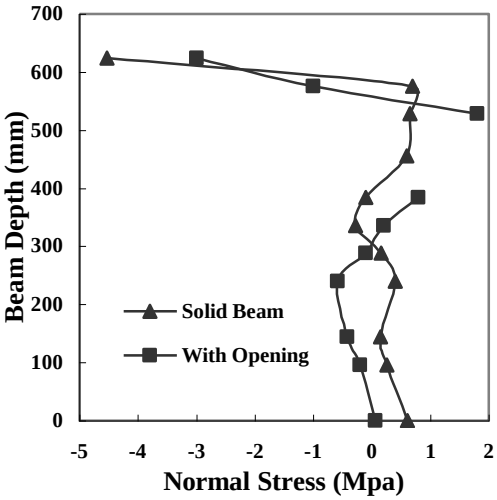


Fig. (44) Shear Stress for Beam S2 at Opening Layout No.2

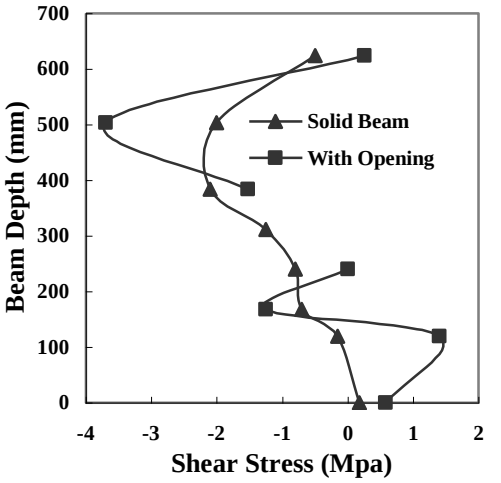


Fig. (45) Shear Stress for Beam S1 at Opening Layout No.3

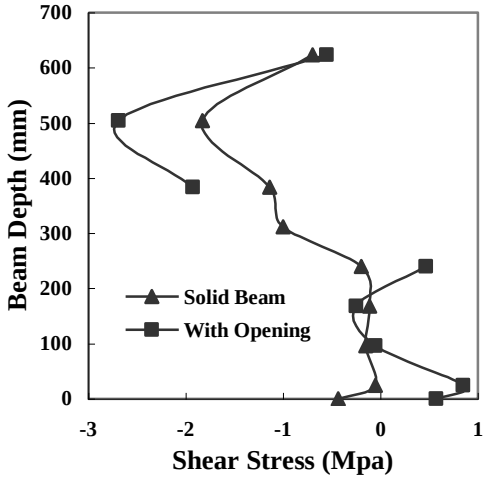


Fig. (46) Shear Stress for Beam S2 at Opening Layout No.3

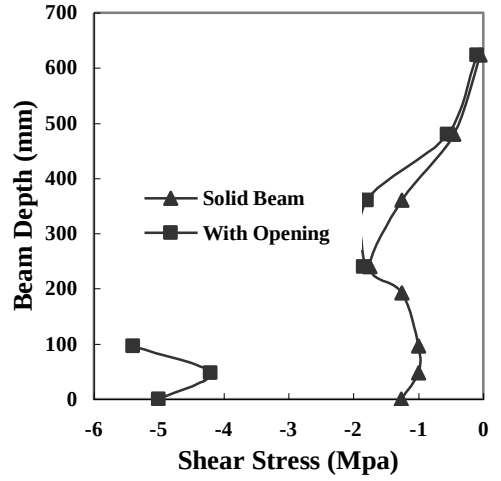


Fig. (47) Shear Stress for Beam S1 at Opening Layout No.4

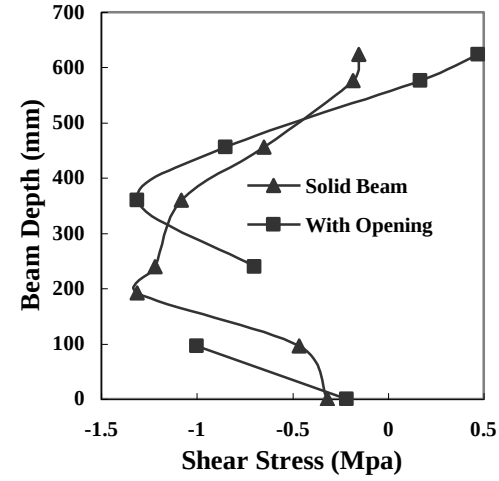


Fig. (48) Shear Stress for Beam S2 at Opening Layout No.4

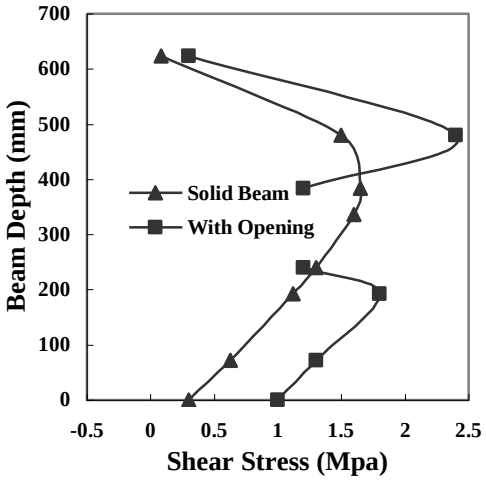


Fig. (49) Shear Stress for Beam S1 at Opening Layout No.5

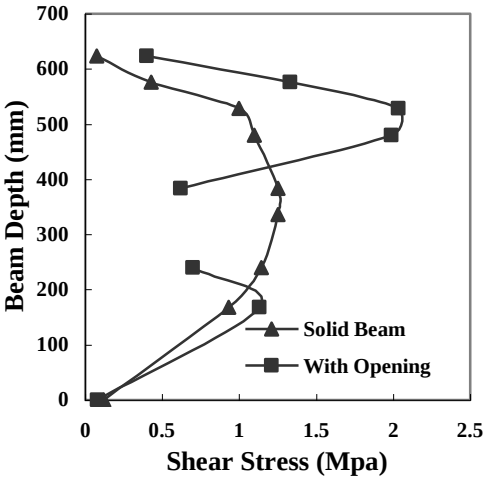


Fig. (50) Shear Stress for Beam S2 at Opening Layout No.5

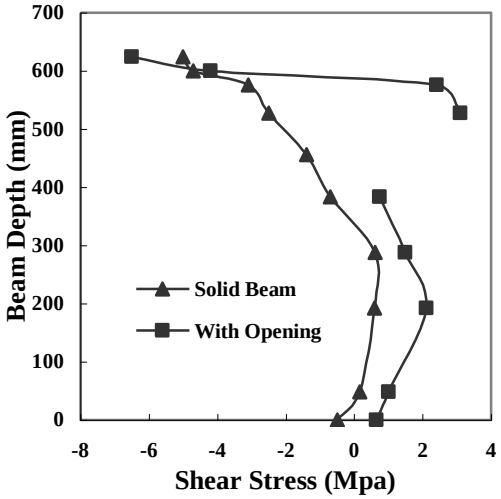


Fig. (51) Shear Stress for Beam S1 at Opening Layout No.2 After Crack

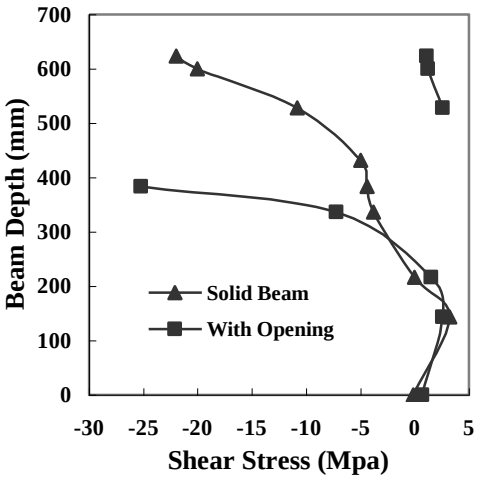


Fig. (52) Shear Stress for Beam S2 at Opening Layout No.2 After Crack

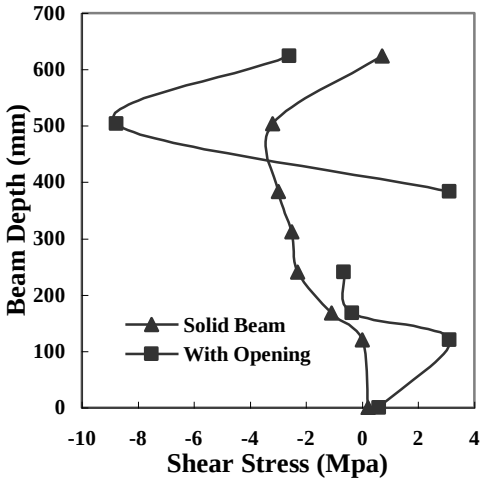


Fig. (53) Shear Stress for Beam S1 at Opening Layout No.3 After Crack

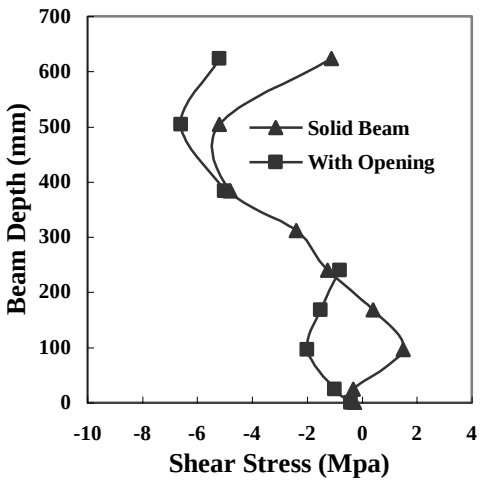


Fig. (54) Shear Stress for Beam S2 at Opening Layout No.3 After Crack

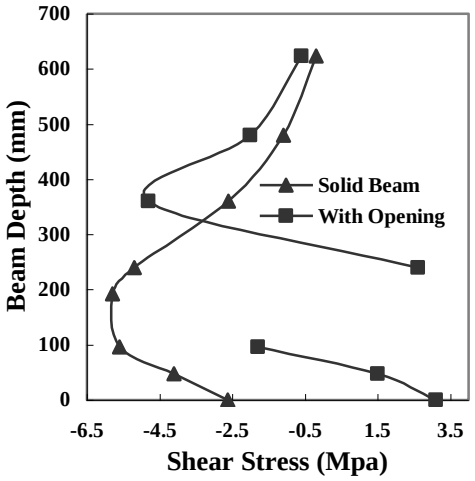


**Fig. (55) Shear Stress for Beam S1 at Opening Layout No.4 After Crack**

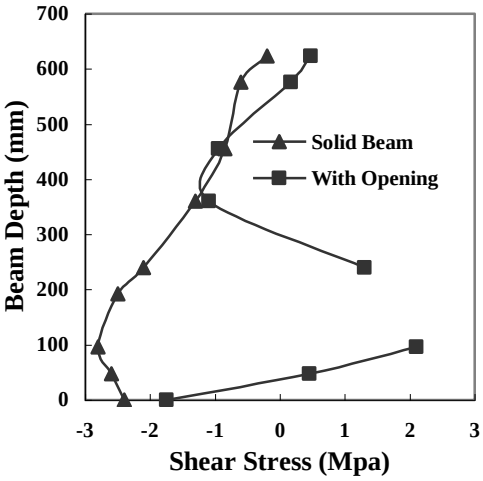


**Fig. (56) Shear Stress for Beam S2 at Opening Layout No.4 After Crack**

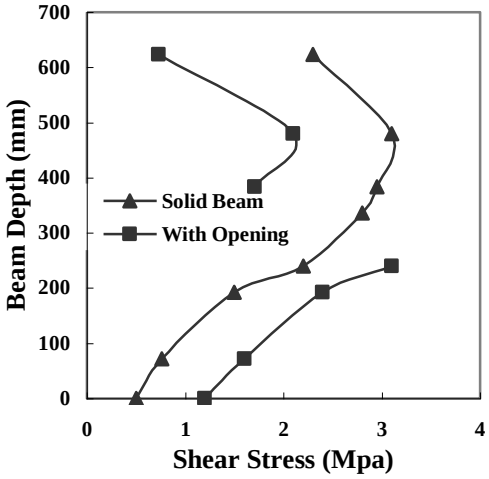


**Fig. (57) Shear Stress for Beam S1 at Opening Layout No.5 After Crack**

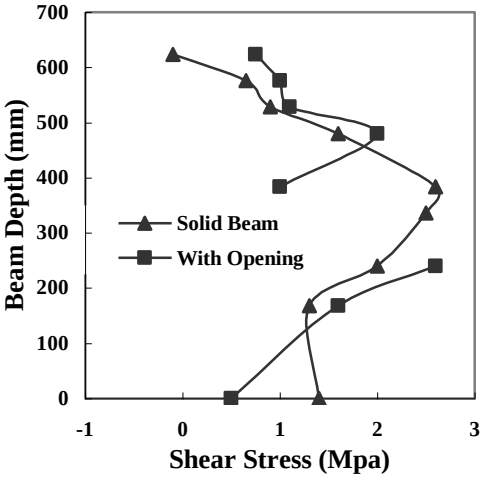


**Fig. (58) Shear Stress for Beam S2 at Opening Layout No.5 After Crack**

**Table (1) Material Properties Used in The Analysis of The Two Deep Beams.**

| Material | Property | Beam S1 | Beam S2 |
|---|---|---|---|
| Reinforcing Steel | Yield Strength (MPa) | 470 | 470 |
| | Young's Modulus (MPa) | $200 \times 10^3$ | $200 \times 10^3$ |
| | Poisson's Ratio | 0.3 | 0.3 |
| | Area: | | |
| | Top Reinforcement | 2Ø10 + 2Ø12 | 2Ø10 + 2Ø12 |
| | Middle Reinforcement | 4 Ø 8 | 4 Ø 8 |
| | Bottom Reinforcement | 2 Ø 12 | 2 Ø 12 |
| Stirrups | Yield Strength (MPa) | - | 355 |
| | Young's Modulus (MPa) | - | $195 \times 10^3$ |
| | Poisson's Ratio | - | 0.3 |
| Concrete | Compressive Strength (MPa) | 39 | 31 |
| | Tensile Strength (MPa) | 3.1 | 2.6 |